J. Fluid Mech. (1990), *vol.* 217, *pp.* 595–613
Printed in Great Britain

Harbour excitations by incident wave groups

By JIANG-KANG WU† AND PHILIP L.-F. LIU

Joseph DeFrees Hydraulics Laboratory, School of Civil and Environmental Engineering, Cornell University, Ithaca, NY 14853, USA

(Received 21 March 1989 and in revised form 30 January 1990)

By using the multiple-scales perturbation method, analytical solutions are obtained for the second-order low-frequency oscillations inside a rectangular harbour excited by incident wave groups. The water depth is a constant. The width of the harbour entrance is of the same order of magnitude as the wavelength of incident carrier (short) waves, but small in comparison with the wavelength of the wave envelope. Because of the modulations in the wave envelope, a second-order long wave is locked in with the wave envelope and propagates with the speed of the group velocity. Outside the harbour, locked long waves also exist in the reflected wave groups, but not in the radiated wave groups. Inside the harbour, the analytical expressions for the locked long waves are obtained. Owing to the discontinuity of the locked long waves across the harbour mouth, second-order free long waves are generated. The free long waves propagate with a speed of $(gh)^{\frac{1}{2}}$ inside and outside the harbour. The free long waves inside the harbour may be resonated in a low-frequency range which is relevant to the harbour resonance.

1. Introduction

Large-amplitude harbour oscillations could create unacceptable vessel movements and excessive mooring forces leading to the breaking of mooring lines. The typical natural periods of a reasonable sized harbour or a moored vessel are of the order of magnitude of minutes. Therefore, they are not excited directly by the wind waves, since typical wind wave periods are of the order of magnitude of seconds. However, sea waves tend to travel in groups whose periods could be much longer than those of the carrier waves. Through nonlinearity second-order long waves exist under these wave groups (Longuet-Higgins & Stewart 1962). These long waves are more relevant to harbour resonances.

Bowers (1977) studied the mean free-surface oscillations in a narrow rectangular channel of constant depth and a discontinuous width; the length of the narrower-width section is finite and the wider section infinite. A train of sinusoidal modulated wave groups incident from infinity generates not only locked long waves but also free long waves. The speed and the direction of the free long waves are not directly associated with the wave groups. Bowers (1977) showed that the free long waves are generated because of the difference in the second-order mean free-surface displacements associated with the locked long waves across the junction of two channels. The free long waves can be resonated inside the narrow channel. The free long waves can also be generated by the refraction of wave groups over an uneven bottom (Molin 1982; Mei & Benmoussa 1984; Liu 1989) or a shear current (Liu,

† Present address: Ocean Engineering Program, Texas A&M University, College Station, TX 77843, USA.

Dingemans & Kostense 1990) and through the scattering of wave groups by a vertical cylinder (Zhou & Liu 1987) or a depth discontinuity (Agnon & Mei 1988).

Recently, Mei & Agnon (1989) studied the long-wave oscillation induced by incident wave groups inside a rectangular harbour. The harbour basin is exposed to the ocean without any protection. The harbour entrance was assumed to be much wider than the short wavelength, but much smaller than the long wavelength. They obtained the approximate analytical solutions for short waves using the geometric ray theory complemented by the parabolic approximation. They demonstrated that the free long waves can be resonated inside the harbour. In this paper, we use a multiple-scales perturbation method to study a similar problem concerning the wave-group-induced harbour resonance. There are two major differences between the present paper and Mei & Agnon's paper. (i) In the present paper the harbour mouth is assumed to be wider than the short wavelength (but it is not required to be much wider than the short wavelength), therefore the short waves are solved exactly by the diffraction theory (e.g. Miles & Munk 1961). (ii) The harbour basin is assumed to be a rectangle and is protected by a pair of thin breakwaters. To achieve a better understanding of the generation and amplification of long waves, we seek analytical solutions when it is possible. Several further simplifications are made in the analysis: (i) the depth is a constant, (ii) the coastline is a straight line and vertically walled, and (iii) energy dissipation is ignored. Under these assumptions, the analytical solutions for the first-order carrier waves are available (e.g. Miles & Munk 1961) and are used to compute the forcing functions responsible for the generation of the second-order long waves. The analytical expressions for both locked and free long waves inside and outside the harbour are obtained. From numerical examples it is shown that only the free long waves are resonated at low frequencies; the locked long waves may be ignored for practical purposes. In the higher frequency range both locked and free long waves could be resonated.

In the following section the governing equations, boundary conditions and the multiple-scale perturbation method are summarized. The first-order, first-harmonic solutions are given in §3. In §4, the second-order wave field is derived. As a special case of the rectangular harbour, the general solutions are reduced to the case of a narrow bay. Numerical results for the incident wave group which consists of two short-wave components are discussed in §5.

2. Formulation of the problem

Consider a rectangular harbour basin connected to a straight line coast. As shown in figure 1, the width of the harbour is B and the length is L. These horizontal dimensions are assumed to be much longer than the typical wavelength of incident short waves. The width of the harbour entrance is denoted as $2a$ and is assumed to be of the same order of magnitude as the wavelength of the carrier waves. The water depth, h, is a constant in the entire region and is of the same order of magnitude as the wavelength of the short waves. Assuming that the water is inviscid and the flow is irrotational, the velocity potential Φ can be introduced and it must satisfy the following governing equation and boundary conditions:

$$\frac{\partial^2 \Phi}{\partial x^2}+\frac{\partial^2 \Phi}{\partial y^2}+\frac{\partial^2 \Phi}{\partial z^2}=0 \quad (-h<z<0), \tag{2.1}$$

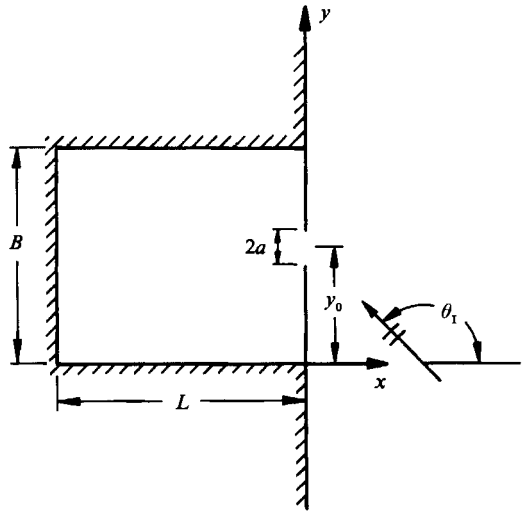

FIGURE 1. A sketch of a rectangular harbour.

$$\frac{\partial \Phi}{\partial z} = 0 \quad (z = -h), \tag{2.2}$$

$$\frac{\partial \zeta}{\partial t} + \frac{\partial \zeta}{\partial x}\frac{\partial \Phi}{\partial z} + \frac{\partial \zeta}{\partial y}\frac{\partial \Phi}{\partial y} = \frac{\partial \Phi}{\partial z} \quad (z = \zeta), \tag{2.3}$$

$$\frac{\partial \Phi}{\partial t} + g\zeta + \frac{1}{2}\left[\left|\frac{\partial \Phi}{\partial x}\right|^2 + \left|\frac{\partial \Phi}{\partial y}\right|^2 + \left|\frac{\partial \Phi}{\partial z}\right|^2\right] = 0 \quad (z = \zeta), \tag{2.4}$$

where $z = \zeta(x, y, t)$ represents the free-surface displacement. The normal velocity component along the solid walls, such as the vertical walls of the harbour basin and the coastline, must vanish.

The incident wave groups propagate with an angle, θ_I, and the wave envelope is colinear with the carrier waves, which have a dominant wave frequency ω. The envelope modulates slowly in both space and time. We assume that the wave slope of the carrier waves is of $O(\epsilon) \ll 1$. The time- and lengthscale of the wave envelope are $O(\epsilon^{-1})$ times those of the carrier waves. It is, therefore, convenient to use the following slow variables:

$$(X, Y) = (\epsilon x, \epsilon y), \quad T = \epsilon t. \tag{2.5}$$

We seek the perturbation solutions:

$$\Phi = \sum_{n=1}^{\infty} \sum_{m=-n}^{n} \epsilon^n \Phi_{(n,m)}(\boldsymbol{x}, z, \boldsymbol{X}, T)\, \mathrm{e}^{-\mathrm{i}m\omega t}, \tag{2.6}$$

$$\zeta = \sum_{n=1}^{\infty} \sum_{m=-n}^{n} \epsilon^n \zeta_{(n,m)}(\boldsymbol{x}, \boldsymbol{X}, T)\, \mathrm{e}^{-\mathrm{i}m\omega t}, \tag{2.7}$$

in which $\zeta_{(n,-m)}$ and $\Phi_{(n,-m)}$ are the complex conjugates of $\zeta_{(n,m)}$ and $\Phi_{(n,m)}$, respectively, $\boldsymbol{x} = (x, y)$, and $\boldsymbol{X} = (X, Y)$.

Substitution of (2.6) and (2.7) into the governing equations, (2.1)–(2.4), yields a set of equations for $\zeta_{(n,m)}$ and $\Phi_{(n,m)}$. Symbolically, these equations can be expressed as

$$\left(\frac{\partial^2}{\partial x^2}+\frac{\partial^2}{\partial y^2}+\frac{\partial^2}{\partial z^2}\right)\Phi_{(n,m)} = F_{(n,m)} \quad (-h < z < 0), \tag{2.8}$$

$$\left(\frac{\partial}{\partial z}-\frac{m^2\omega^2}{g}\right)\Phi_{(n,m)} = G_{(n,m)} \quad (z = 0), \tag{2.9}$$

$$\frac{\partial}{\partial z}\Phi_{(n,m)} = 0 \quad (z = -h). \tag{2.10}$$

The free-surface boundary conditions have been linearized and are evaluated at $z = 0$. The functions $F_{(n,m)}$ and $G_{(n,m)}$ are expressed in terms of solutions of order lower than n. Their explicit forms can be found in Zhou & Liu (1987) and are also given in the following sections when they are needed. The no-flux boundary condition along the solid boundaries requires

$$\frac{\partial}{\partial \boldsymbol{n}}\Phi_{(n,m)} = 0 \quad \text{on the solid boundaries,} \tag{2.11}$$

where $\boldsymbol{n}$ denotes the unit normal along the solid boundaries.

3. The first-order short-wave solutions

The first-order solutions contain two components: the first-harmonic (short wave) component, $\Phi_{(1,1)}$, and the low-frequency modulation component, $\Phi_{(1,0)}$. The governing equations for the first-harmonic potential are the well-known linearized boundary-value problem:

$$\left(\frac{\partial^2}{\partial x^2}+\frac{\partial^2}{\partial y^2}+\frac{\partial^2}{\partial z^2}\right)\Phi_{(1,1)} = 0 \quad (-h < z < 0), \tag{3.1}$$

$$\left(\frac{\partial}{\partial z}-\frac{\omega^2}{g}\right)\Phi_{(1,1)} = 0 \quad (z = 0), \tag{3.2}$$

$$\frac{\partial}{\partial z}\Phi_{(1,1)} = 0 \quad (z = -h), \tag{3.3}$$

$$\frac{\partial}{\partial y}\Phi_{(1,1)} = 0 \quad (-L < x < 0, \quad y = 0 \text{ and } B), \tag{3.4}$$

$$\frac{\partial}{\partial x}\Phi_{(1,1)} = 0, \quad \begin{cases} x = -L, & 0 < y < B, \\ x = 0+, & |y-y_0| > a, \\ x = 0-, & |y-y_0| > a, \quad 0 < y < B, \end{cases} \tag{3.5}$$

where $x = 0+$ denotes the shoreline, while $x = 0-$ represents the harbour side of the solid boundary. The scattered waves must be outgoing waves at infinity ($x > 0$, $r \to \infty$).

The incident first-harmonic wave potential is the superposition of N pairs of

colinear short waves with wavenumbers $k \pm \epsilon n k_0$ and wave frequencies $\omega \pm \epsilon n \omega_0$ ($n = 1, 2, 3, \ldots, N$; provided that $\epsilon N \ll 1$). Thus

$$\Phi^{\mathrm{I}}_{(1,1)} = \frac{ig}{\omega} f(z) A^{\mathrm{I}} \exp(\mathrm{i}\psi^{\mathrm{I}}), \tag{3.6}$$

with

$$f(z) = \frac{\cosh k(z+h)}{\cosh kh}, \quad \omega^2 = gk \tanh kh, \tag{3.7}$$

$$\psi^{\mathrm{I}} = k(x \cos\theta_{\mathrm{I}} + y \sin\theta_{\mathrm{I}}), \tag{3.8}$$

and the incident wave envelope is a function of the slow variables (X, T),

$$A^{\mathrm{I}} = A(\Psi^{\mathrm{I}} - \omega_0 T) = \sum_{n=-N}^{N} A^{\mathrm{I}}_n \exp[in(\Psi^{\mathrm{I}} - \omega_0 T)], \tag{3.9}$$

where

$$\Psi^{\mathrm{I}} = k_0(X \cos\theta_{\mathrm{I}} + Y \sin\theta_{\mathrm{I}}), \quad C_g = \frac{\omega_0}{k_0}, \tag{3.10}$$

and A^{I}_n ($n = \pm 1, \pm 2, \pm 3, \ldots, \pm N$) are constants.

For monochromatic waves (i.e. $A^{\mathrm{I}} = \text{constant}$), the procedure for obtaining analytical solutions for the wave potential governed by (3.1)–(3.5) has been outlined by Miles & Munk (1961). Because the boundary-value problem for the first-harmonic potential is a linear one, the solutions subject to the incident wave groups defined in (3.6) can be readily obtained from the solutions for monochromatic waves by using the principle of superposition.

Outside the harbour the first-harmonic potential can be decomposed into the incident wave, the reflected wave, and the radiated wave potentials:

$$\Phi^{0}_{(1,1)} = \frac{ig}{\omega} f(z)[A^{\mathrm{I}} \exp(\mathrm{i}\psi^{\mathrm{I}}) + A^{\mathrm{r}} \exp(\mathrm{i}\psi^{\mathrm{r}}) + \phi^{\mathrm{s}}], \tag{3.11}$$

where A^{r} and ψ^{r} are the reflected wave envelope and the associated phase function,

$$A^{\mathrm{r}} = \sum_{n=-N}^{N} A^{\mathrm{I}}_n \exp[in(\Psi^{\mathrm{r}} - \omega_0 T)], \tag{3.12}$$

$$\psi^{\mathrm{r}} = k(-x \cos\theta_{\mathrm{I}} + y \sin\theta_{\mathrm{I}}), \tag{3.13}$$

in which

$$\Psi^{\mathrm{r}} = k_0(-X \cos\theta_{\mathrm{I}} + Y \sin\theta_{\mathrm{I}}). \tag{3.14}$$

Note that the reflected wave envelope propagates in the same direction as the reflected short waves. The no-flux boundary condition along the shoreline, $x = 0$, is satisfied by the sum of the incident and reflected wave potentials. The radiated waves can be expressed as

$$\phi^{\mathrm{s}} = \sum_{n=-N}^{N} A^{\mathrm{I}}_n \int_m (-\tfrac{1}{2}\mathrm{i}) H^{(1)}_0(kr)\, U_n(\eta)\, \mathrm{d}\eta \exp[in(k_0 R - \omega_0 T)], \tag{3.15}$$

with

$$R = [X^2 + (Y - \epsilon y_0)^2]^{\frac{1}{2}}, \quad r = [x^2 + (y-\eta)^2]^{\frac{1}{2}}, \quad \int_m \mathrm{d}\eta = \int_{y_0-a}^{y_0+a} \mathrm{d}\eta, \tag{3.16}$$

where $U_n(\eta)$ is the first-order normal velocity along the harbour mouth, and $H^{(1)}_0$ is the Hankel function of the first kind and zeroth order. The radiation condition is satisfied by the radiated waves.

Inside the harbour the first-harmonic wave potential can be expressed in terms of the Green's function for the rectangular basin with the normal velocity $U_n(\eta)$ across the harbour mouth. Thus,

$$\Phi^{\mathrm{H}}_{(1,1)} = \frac{\mathrm{i}g}{\omega} f(z) \sum_{q=0}^{\infty} \{A_{q1} \exp[\mathrm{i}k_q(x+L)] + A_{q2} \exp[-\mathrm{i}k_q(x+L)]\} \cos(\beta_q y) \quad (-L < x < 0, \quad 0 < y < B), \tag{3.17}$$

with

$$\beta_q = \frac{q\pi}{B}, \quad k_q = (k^2 - \beta_q^2), \tag{3.18}$$

where k_q could be either a real or an imaginary number; the real values correspond to the propagating modes and the imaginary values represent the evanescent modes. For convenience, we order the values of k_q in such way that the first Q-numbers are real and the rest of them are imaginary. In (3.17) A_{q1} and A_{q2} are slowly varying functions and are related to each other through the no-flux boundary condition at $x = L$:

$$A_{q1} = -\sum_{n=-N}^{N} \frac{\epsilon_q \mathscr{G}_q(\kappa_n) A^{\mathrm{I}}_n}{k_{qn} B \sin(k_{qn} L)} \exp\{\mathrm{i}n[k_{0q}(X+\epsilon L) - \omega_0 T]\}, \tag{3.19}$$

$$A_{q2} = -\sum_{n=-N}^{N} \frac{\epsilon_q \mathscr{G}_q(\kappa_n) A^{\mathrm{I}}_n}{k_{qn} B \sin(k_{qn} L)} \exp\{-\mathrm{i}n[k_{0q}(X+\epsilon L) + \omega_0 T]\}, \tag{3.20}$$

where

$$\mathscr{G}_q(\kappa_n) = \int_m \cos(\beta_q \eta)\, U_n(\eta)\, \mathrm{d}\eta, \tag{3.21}$$

$$k_{qn} = (\kappa_n^2 - \beta_q^2)^{\frac{1}{2}} = k_q + n\epsilon k_{0q} + O(\epsilon^2), \quad \kappa_n = k + \epsilon n k_0, \quad k_{0q} = \frac{k k_0}{k_q}, \tag{3.22}$$

and $\epsilon_m = 1$, for $m = 0$, and $\epsilon_m = 2$, for $m \geqslant 1$.

To complete the first-order and first-harmonic solution, one has to find the normal velocity distribution across the harbour mouth, $U_n(\eta)$. Requiring the free-surface displacement to be continuous across the mouth of the harbour, the following integral equation is obtained (Miles & Munk 1961):

$$\int_m \mathscr{K}_n(y, \eta)\, U_n(\eta)\, \mathrm{d}\eta = 2A^{\mathrm{I}}_n \exp[\mathrm{i}(\kappa_n y \sin\theta_{\mathrm{I}})], \tag{3.23}$$

for the nth component, where the kernel function is

$$\mathscr{K}_n(y, \eta) = -\sum_{m=0}^{\infty} \frac{\epsilon_m \cot(k_{mn} L)}{k_{mn} B} \cos(\beta_m y) \cos(\beta_m \eta) + \tfrac{1}{2}\mathrm{i} H_0^{(1)}(\kappa_n |y - \eta|). \tag{3.24}$$

The integral equation (3.23) can be solved numerically for a given set of wave parameters and harbour geometry.

4. Long waves and mean free-surface displacement

In this section the solutions for the long wave $\Phi_{(1,0)}$ and the corresponding second-order dynamic free-surface displacement $\zeta_{(2,0)}$ are presented. The governing equations for $\Phi_{(1,0)}$ can be written as

$$\frac{\partial^2 \Phi_{(1,0)}}{\partial T^2} - gh\left(\frac{\partial^2 \Phi_{(1,0)}}{\partial X^2} + \frac{\partial^2 \Phi_{(1,0)}}{\partial Y^2}\right) = \mathrm{L}[\overline{\Phi_{(1,1)}}], \tag{4.1}$$

with

$$\mathrm{L}[\overline{\Phi_{(1,1)}}] = \frac{\partial}{\partial X}\overline{\left[\mathrm{i}\omega\Phi_{(1,1)}\frac{\partial}{\partial x}\Phi_{(1,-1)}+*\right]}+\frac{\partial}{\partial Y}\overline{\left[\mathrm{i}\omega\Phi_{(1,1)}\frac{\partial}{\partial y}\Phi_{(1,-1)}+*\right]}$$

$$-\frac{\partial}{\partial T}\overline{\left[\left|\frac{\partial}{\partial x}\Phi_{(1,1)}\right|^2+\left|\frac{\partial}{\partial y}\Phi_{(1,1)}\right|^2+\left|\frac{\partial}{\partial z}\Phi_{(1,1)}\right|^2-\frac{\omega^2}{g}\left(\Phi_{(1,1)}\frac{\partial}{\partial z}\Phi_{(1,-1)}+*\right)\right]} \quad (z=0), \tag{4.2}$$

where $*$ denotes the complex conjugate of the preceding term, and the overbar in (4.1) distinguishes the self-products of the propagating waves from the rest (Agnon & Mei 1985). The forcing terms in (4.1) are functions of the slow variables only. Once $\Phi_{(1,0)}$ is solved, the corresponding free-surface displacement can be calculated from the time-averaged Bernoulli equation on the still water level:

$$\zeta_{(2,0)} = -\frac{1}{g}\left[\frac{\partial}{\partial T}\Phi_{(1,0)}+\overline{\left|\frac{\partial}{\partial x}\Phi_{(1,1)}\right|^2}+\overline{\left|\frac{\partial}{\partial y}\Phi_{(1,1)}\right|^2}+\overline{\left|\frac{\partial}{\partial z}\Phi_{(1,1)}\right|^2}\right.$$

$$\left.-\frac{\omega^2}{g}\overline{\left(\Phi_{(1,1)}\frac{\partial}{\partial z}\Phi_{(1,-1)}+*\right)}\right] \quad (z=0). \tag{4.3}$$

Now consider the forcing functions in (4.1). On the ocean side, $x > 0$, the first-order, first-harmonic wave potential is made up of the incident wave potential, $\Phi^{\mathrm{I}}_{(1,1)}$, the reflected wave potential, $\Phi^{\mathrm{r}}_{(1,1)}$, and the radiated wave potential, $\Phi^{\mathrm{s}}_{(1,1)}$, as defined in (3.11). Only the self-products of each wave component contribute to the forcing functions. Thus,

$$\mathrm{L}[\overline{\Phi_{(1,1)}}] = \mathrm{L}[\overline{\Phi^{\mathrm{I}}_{(1,1)}}]+\mathrm{L}[\overline{\Phi^{\mathrm{r}}_{(1,1)}}]+\mathrm{L}[\overline{\Phi^{\mathrm{s}}_{(1,1)}}], \tag{4.4}$$

with

$$\mathrm{L}[\overline{\Phi^{\mathrm{I}}_{(1,1)}}] = \mathfrak{G}\frac{\partial}{\partial X^{\mathrm{I}}}|A^{\mathrm{I}}|^2, \tag{4.5}$$

$$\mathrm{L}[\overline{\Phi^{\mathrm{r}}_{(1,1)}}] = \mathfrak{G}\frac{\partial}{\partial X^{\mathrm{r}}}|A^{\mathrm{r}}|^2, \tag{4.6}$$

$$\mathrm{L}[\overline{\Phi^{\mathrm{s}}_{(1,1)}}] = 0, \tag{4.7}$$

where

$$\mathfrak{G} = \frac{g^2k^2}{\omega^2}\left(2\frac{\omega}{k}+\frac{C_{\mathrm{g}}}{\cosh^2 kh}\right), \tag{4.8}$$

in which $X^{\mathrm{I}} = \Psi^{\mathrm{I}}/k_0$ and $X^{\mathrm{r}} = \Psi^{\mathrm{r}}/k_0$ denote the directions of the incident and the reflected wave propagation, respectively. The radiated waves propagate in the radial direction and their amplitudes decay as $r^{-\frac{1}{2}}$ as r becomes large. The self-products of the radiated waves are functions of the fast variables. Therefore, the radiated waves do not contribute to the forcing functions for the long waves (Zhou & Liu 1987).

The long waves in the ocean can be decomposed into the locked long waves propagating with the incident wave envelope $\tilde{\Phi}^{\mathrm{I}}_{(1,0)}$, the locked long waves associated with the reflected wave groups, $\tilde{\Phi}^{\mathrm{r}}_{(1,0)}$, and the free long waves, $\hat{\Phi}^{0}_{(1,0)}$. Hence,

$$\Phi^{0}_{(1,0)} = \tilde{\Phi}^{\mathrm{I}}_{(1,0)}+\tilde{\Phi}^{\mathrm{r}}_{(1,0)}+\hat{\Phi}^{0}_{(1,0)}, \tag{4.9}$$

where

$$\frac{\partial^2\tilde{\Phi}^{\mathrm{I}}_{(1,0)}}{\partial T^2}-gh\frac{\partial^2\tilde{\Phi}^{\mathrm{I}}_{(1,0)}}{\partial(X^{\mathrm{I}})^2} = \mathfrak{G}\frac{\partial}{\partial X^{\mathrm{I}}}|A^{\mathrm{I}}|^2, \tag{4.10}$$

$$\frac{\partial^2\tilde{\Phi}^{\mathrm{r}}_{(1,0)}}{\partial T^2}-gh\frac{\partial^2\tilde{\Phi}^{\mathrm{r}}_{(1,0)}}{\partial(X^{\mathrm{r}})^2} = \mathfrak{G}\frac{\partial}{\partial X^{\mathrm{r}}}|A^{\mathrm{r}}|^2, \tag{4.11}$$

and

$$\frac{\partial^2\hat{\Phi}^{0}_{(1,0)}}{\partial T^2}-gh\left(\frac{\partial^2\hat{\Phi}^{0}_{(1,0)}}{\partial X^2}+\frac{\partial^2\hat{\Phi}^{0}_{(1,0)}}{\partial Y^2}\right) = 0. \tag{4.12}$$

We integrate (4.10) and (4.11) to obtain

$$\tilde{\Phi}^{\mathrm{I}}_{(1,0)} = \frac{\mathfrak{G}}{C_{\mathrm{g}}^2 - gh}\left\{-\frac{\mathrm{i}}{k_0}\sum_{n=1}^{2N}\frac{C_n}{n}\exp\left[\mathrm{i}n(\Psi^{\mathrm{I}} - \omega_0 T)\right] + * + C_0(X^{\mathrm{I}} - C_{\mathrm{g}} T)\right\}, \tag{4.13}$$

$$\tilde{\Phi}^{\mathrm{r}}_{(1,0)} = \frac{\mathfrak{G}}{C_{\mathrm{g}}^2 - gh}\left\{-\frac{\mathrm{i}}{k_0}\sum_{n=1}^{2N}\frac{C_n}{n}\exp\left[\mathrm{i}n(\Psi^{\mathrm{r}} - \omega_0 T)\right] + * + C_0(X^{\mathrm{r}} - C_{\mathrm{g}} T)\right\}, \tag{4.14}$$

where

$$|A^{\mathrm{I}}|^2 = \sum_{n=1}^{2N} C_n \exp\left[\mathrm{i}n(\Psi^{\mathrm{I}} - \omega_0 T)\right] + * + C_0. \tag{4.15}$$

In (4.13) and (4.14) the linear terms in X^{I} and X^{r} represent the steady currents associated with the incident and reflected waves, while the terms linear in T contribute to the steady mean free-surface set-down.

The free long waves outside the harbour can be written as

$$\hat{\Phi}^0_{(1,0)} = \frac{\mathfrak{G}}{C_{\mathrm{g}}^2 - gh}\left\{C^0 \ln R + D^0 T + \sum_{n=1}^{2N}\xi_n \exp\left(-\mathrm{i}n\omega_0 T\right) \times \int_{m_0} G(X, Y; \xi = 0, \eta)\, V(\eta)\, \mathrm{d}\eta + *\right\}, \tag{4.16a}$$

with

$$\int_{m_0} \mathrm{d}\eta = \int_{\epsilon(y_0 - a)}^{\epsilon(y_0 + a)} \mathrm{d}\eta, \quad R^2 = X^2 + Y^2. \tag{4.16b}$$

In (4.16a) C^0 and D^0 represent the steady current and the steady set-down associated with the free long waves and $G(X, Y; \xi, \eta)$ is the Green's function for the wave equation, (4.12), associated with a periodic point source/sink located at (ξ, η) with a frequency $n\omega_0$. The Green's function can be expressed as

$$G(X, Y; \xi = 0, \eta) = -\tfrac{1}{2}\mathrm{i}H_0^{(1)}(n\alpha k_0 \mathscr{R}), \tag{4.17}$$

with

$$\mathscr{R} = [X^2 + (Y - \eta)^2]^{\frac{1}{2}}, \tag{4.18}$$

$$\alpha = C_{\mathrm{g}}(gh)^{-\frac{1}{2}}. \tag{4.19}$$

In (4.16a) $V(\eta)$ represents the normal velocity, associated with the long waves, across the harbour entrance. For later use, we record the velocity potential for the free long waves and the corresponding flux across the harbour mouth here:

$$\hat{\Phi}^0_{(1,0)} = \frac{\mathfrak{G}}{C_{\mathrm{g}}^2 - gh}\left\{C^0 \ln R + D^0 T + \sum_{n=1}^{2N}\xi_n \exp\left(-\mathrm{i}n\omega_0 T\right) \times \int_{m_0} -\tfrac{1}{2}\mathrm{i}\left[1 + \frac{2\mathrm{i}}{\pi}\ln\left(\tfrac{1}{2}\nu n\alpha k_0 |Y - \eta|\right)\right] V(\eta)\, \mathrm{d}\eta + *\right\}, \tag{4.20}$$

$$\lim_{R \to 0}\left(\pi R \frac{\partial \hat{\Phi}^0_{(1,0)}}{\partial R}\right) = \frac{\mathfrak{G}}{C_{\mathrm{g}}^2 - gh}\sum_{n=1}^{2N}\xi_n \exp\left(-\mathrm{i}n\omega_0 T\right) + * + C^0, \tag{4.21}$$

where the width of the harbour entrance has been assumed to be much smaller than the wavelength of the incident wave envelope. Note that the velocity $V(\eta)$ has been scaled in such a way that total flux across the harbour mouth is unity. The amplitudes of the free long waves, ξ_n, in (4.16) need to be determined.

The long waves inside the harbour can also be decomposed into locked long waves and free long waves, i.e.

$$\Phi^{\mathrm{H}}_{(1,0)} = \tilde{\Phi}^{\mathrm{H}}_{(1,0)} + \hat{\Phi}^{\mathrm{H}}_{(1,0)}, \tag{4.22}$$

where

$$\frac{\partial^2 \tilde{\Phi}^{\mathrm{H}}_{(1,0)}}{\partial T^2} - gh\left(\frac{\partial^2 \tilde{\Phi}^{\mathrm{H}}_{(1,0)}}{\partial X^2} + \frac{\partial^2 \tilde{\Phi}^{\mathrm{H}}_{(1,0)}}{\partial Y^2}\right) = \mathrm{L}[\overline{\Phi^{\mathrm{H}}_{(1,1)}}], \tag{4.23}$$

$$\frac{\partial^2 \hat{\Phi}^{\mathrm{H}}_{(1,0)}}{\partial T^2} - gh\left(\frac{\partial^2 \hat{\Phi}^{\mathrm{H}}_{(1,0)}}{\partial X^2} + \frac{\partial^2 \hat{\Phi}^{\mathrm{H}}_{(1,0)}}{\partial Y^2}\right) = 0. \tag{4.24}$$

The first-order, first-harmonic waves inside the harbour basin, given in (3.17)–(3.24), consist of two sets of progressive waves propagating in the $\pm x$-directions and evanescent modes. The amplitudes of the progressive waves oscillate in the y-direction. Similar to the situation outside the harbour, only the propagation modes contribute to the forcing functions for the long waves. Therefore,

$$\mathrm{L}(\overline{\Phi^{\mathrm{H}}_{(1,1)}}) = \sum_{q=0}^{Q} [\mathrm{L}(\overline{\phi_{q1}}) + \mathrm{L}(\overline{\phi_{q2}})] \quad (z = 0), \tag{4.25}$$

where

$$\phi_{q1} = \frac{\mathrm{i}g}{\omega} f(z) A_{q1} \exp[\mathrm{i}k_q(x+L)] \cos(\beta_q y), \tag{4.26a}$$

$$\phi_{q2} = \frac{\mathrm{i}g}{\omega} f(z) A_{q2} \exp[-\mathrm{i}k_q(x+L)] \cos(\beta_q y). \tag{4.26b}$$

Substituting (4.25) and (4.26) into the operator, $\overline{\mathrm{L}(\ )}$, defined in (4.2), we obtain, after some algebraic manipulations,

$$\overline{\mathrm{L}(\Phi^{\mathrm{H}}_{(1,1)})} = \sum_{q=0}^{Q} \left(\frac{2\mathscr{D}_q}{\epsilon_q}\right) \frac{\partial}{\partial X} (|A_{q1}|^2 - |A_{q2}|^2), \tag{4.27}$$

where

$$\mathscr{D}_q = \frac{g^2 k_q}{2\omega^2} [2\omega + kC_{\mathrm{g}}(1-\gamma^2)], \quad \gamma = \tanh kh. \tag{4.28}$$

The locked long waves inside the harbour can now be obtained by integrating (4.23) with (4.27):

$$\tilde{\Phi}^{\mathrm{H}}_{(1,0)} = \sum_{q=0}^{Q} \sum_{n=1}^{2N} \left\{ -\mathrm{i} \frac{2\mathscr{D}_q}{k_{0q}\epsilon_q} \frac{2p_{qn}}{(C_{\mathrm{g}}^2 - gh)\, n} \cos[nk_{0q}(X+\epsilon L)] \exp(-\mathrm{i}n\omega_0 T) + * \right\} + \tilde{D}T, \tag{4.29}$$

where

$$\left.\begin{aligned} |A_{q1}|^2 &= \sum_{n=1}^{2N} p_{qn} \exp\{\mathrm{i}n[k_{0q}(X+\epsilon L) - \omega_0 T]\} + * + p_{q0}, \\ C_{\mathrm{g}_q} &= \frac{\omega_0}{k_{0q}} = C_{\mathrm{g}} \frac{k_q}{k}. \end{aligned}\right\} \tag{4.30}$$

Both $\tilde{D}$ and p_{q0} contribute to the steady component of the second-order free-surface displacement. While p_{q0} is a known quantity, $\tilde{D}$ is to be determined. Because the no-flux boundary conditions along the solid walls of the harbour must be satisfied, the steady current at this order is zero. The corresponding free long waves inside the harbour can readily be written in the following form:

$$\hat{\Phi}^{\mathrm{H}}_{(1,0)} = \sum_{n=1}^{2N} \frac{\mathfrak{G}}{C_{\mathrm{g}}^2 - gh} \lambda_{0n} \int_{m_0} G^{\mathrm{H}}_n(X, Y; \eta)\, V(\eta)\, \mathrm{d}\eta \exp(-\mathrm{i}n\omega_0 T) + * + \hat{D}T, \tag{4.31}$$

where
$$G_n^{\mathrm{H}}(X, Y; \eta) = -\sum_{q=0}^{\infty} \frac{\epsilon_q \cos[\mathscr{K}_{qn}(X+\epsilon L)]}{\epsilon B \mathscr{K}_{qn} \sin(\epsilon \mathscr{K}_{qn} L)} \cos(\beta_{0q} Y) \cos(\beta_{0q} \eta),$$
$$\mathscr{K}_{qn} = [(n\alpha k_0)^2 - \beta_{0q}^2]^{\frac{1}{2}}, \quad \beta_{0q} = \frac{q\pi}{\epsilon B}, \tag{4.32}$$

and λ_{0n} is to be determined. The free long waves also satisfy the no-flux boundary conditions along the sidewalls of the harbour basin. The integration constant, $\hat{D}$, which affects the steady component of the second-order free-surface displacement inside the harbour, is also to be determined.

To complete the solutions for the long waves inside and outside the harbour, matching conditions across the harbour mouth must be used. Similar to the first-order, first-harmonic solutions, continuity of the second-order pressure and the second-order flux along the harbour mouth is required:

$$\tilde{\Phi}^{\mathrm{I}}_{(1,0)} + \tilde{\Phi}^{\mathrm{r}}_{(1,0)} + \hat{\Phi}_{(1,0)} = \tilde{\Phi}^{\mathrm{H}}_{(1,0)} + \hat{\Phi}^{\mathrm{H}}_{(1,0)} \quad (X = 0, \quad |Y - \epsilon y_0| < \epsilon a), \tag{4.33}$$

$$\lim_{R \to 0} \left(\pi R \frac{\partial \hat{\Phi}^0_{(1,0)}}{\partial R} \right) = \int_0^{\epsilon B} \frac{\partial}{\partial X} [\tilde{\Phi}^{\mathrm{H}}_{(1,0)} + \hat{\Phi}^{\mathrm{H}}_{(1,0)}] \, \mathrm{d}Y \quad (X = 0), \tag{4.34}$$

in which the fact that the sum of the incident and reflected locked long waves satisfies the no-flux condition along the coastline, $X = 0$, has been used. Substituting (4.21), (4.29), and (4.31) into (4.34), we collect the coefficients for each time harmonic, including the steady component, and obtain

$$\xi_n = \lambda_{0n} + \frac{C_{\mathrm{g}}^2 - gh}{\mathfrak{G}} \sum_{q=0}^{Q} \frac{2\mathscr{D}_q}{\epsilon_q} \frac{2\mathrm{i}Bp_{qn}}{C_{\mathrm{g}_q}^2 - gh} \sin(n\epsilon k_{0q} L) \quad (n = 1, 2, \ldots, 2N) \tag{4.35a}$$

$$C^0 = 0. \tag{4.35b}$$

Substitutions of (4.13), (4.14), (4.29), and (4.35) into (4.33) yield, for the steady component,

$$\tilde{D} + \hat{D} = -\frac{2C_0 C_{\mathrm{g}} \mathfrak{G}}{C_{\mathrm{g}}^2 - gh}, \tag{4.36a}$$

and for the dynamic components the following integral equation for λ_{0n}:

$$\lambda_{0n} \int_{m_0} \mathbb{K}_n(Y, \eta) \, V(\eta) \, \mathrm{d}\eta = \mathbb{W}(Y), \tag{4.36b}$$

with
$$\mathbb{K}_n(Y, \eta) = -\mathrm{i}nk_0 \left\{ \sum_{q=0}^{Q} \frac{\epsilon_q}{\epsilon B \mathscr{K}_{qn}} \cot(\epsilon \mathscr{K}_{qn} L) \cos(\beta_{0q} Y) \cos(\beta_{0q} \eta) \right.$$
$$\left. - \tfrac{1}{2}\mathrm{i} \left[1 + \frac{2\mathrm{i}}{\pi} \ln(\tfrac{1}{2}\nu n \alpha k_0 |Y - \eta|) \right] \right\}, \tag{4.37}$$

$$\mathbb{W}(Y) = 2C_n \exp(\mathrm{i}nk_0 Y \sin\theta_{\mathrm{I}}) - \sum_{q=0}^{Q} \frac{2\mathscr{D}_q}{\epsilon_q} \frac{2p_{qn}}{C_{\mathrm{g}_q}^2 - gh}$$
$$\times \frac{C_{\mathrm{g}}^2 - gh}{\mathfrak{G}} \frac{k_0}{k_{0q}} \cos(n\epsilon k_{0q} L) + \mathrm{i}nk_0 \frac{C_{\mathrm{g}}^2 - gh}{\mathfrak{G}} \sum_{q=0}^{Q} \frac{2\mathscr{D}_q}{\epsilon_q} \sin(n\epsilon k_{0q} L)$$
$$\times \frac{2\mathrm{i}\epsilon B p_{qn}}{C_{\mathrm{g}_q}^2 - gh} \int_{m_0} \left\{ -\tfrac{1}{2}\mathrm{i} \left[1 + \frac{2\mathrm{i}}{\pi} \ln \tfrac{1}{2}(\nu n \alpha k_0 |Y - \eta|) \right] \right\} V(\eta) \, \mathrm{d}\eta. \tag{4.38}$$

The integral equation (4.36*b*) can be solved by a variational method (Miles & Munk 1961) as

$$\lambda_{0n} = \frac{\mathbb{N}_n}{\mathbb{D}_n} = \frac{\int_{m_0} \mathbb{W}(Y)\, V(\eta)\, \mathrm{d}\eta}{\int_{m_0}\int_{m_0} V(Y)\, \mathbb{K}_n(Y,\eta)\, V(\eta)\, \mathrm{d}Y\, \mathrm{d}\eta}. \tag{4.39}$$

For a given velocity distribution, $V(\eta)$, (4.39) may be evaluated.

Assuming that the harbour mouth is small in comparison with the wavelength of the long waves, we can approximate the velocity distribution as

$$V(\eta) = \frac{1}{\pi}[(\epsilon a)^2 - (\epsilon y_0 - \eta)^2]^{-\frac{1}{2}}. \tag{4.40}$$

Equations (4.39) can be written as

$$\begin{aligned}\mathbb{N}_n = {} & 2C_n \exp(\mathrm{i}nk_0 \epsilon y_0 \sin\theta_{\mathrm{I}}) - \sum_{q=0}^{Q} \frac{2\mathscr{D}_q}{\epsilon_q} \frac{2p_{qn}}{C_{\mathrm{g}_q}^2 - gh} \\ & \times \frac{C_{\mathrm{g}}^2 - gh}{\mathfrak{G}} \frac{k_0}{k_{0q}} \cos(n\epsilon k_{0q} L) + \mathrm{i}nk_0 \frac{C_{\mathrm{g}}^2 - gh}{\mathfrak{G}} \sum_{q=0}^{Q} \frac{2\mathscr{D}_q}{\epsilon_q} \\ & \times \frac{2\mathrm{i}\epsilon B p_{qn}}{C_{\mathrm{g}_q}^2 - gh} \sin(n\epsilon k_{0q} L) \left[-\tfrac{1}{2}\mathrm{i} + \frac{1}{\pi} \ln \tfrac{1}{4}(\nu n \epsilon \alpha k_0 a) \right],\end{aligned} \tag{4.41}$$

$$\mathbb{D}_n = -\mathrm{i}nk_0 \left\{ \sum_{q=0}^{\infty} \frac{\epsilon_q}{\epsilon B \mathscr{K}_{qn}} \cot(\epsilon \mathscr{K}_{qn} L) \cos^2(\beta_q y_0)\, J_0^2(\beta_q a) - \tfrac{1}{2}\mathrm{i} \left[1 + \frac{2\mathrm{i}}{\pi} \ln \tfrac{1}{4}(\nu n \epsilon \alpha k_0 a) \right] \right\}. \tag{4.42}$$

The long wave potential, $\Phi_{(1,0)}$, is completed.

The corresponding second-order free-surface displacement can be obtained from (4.3) by using the formulae for $\Phi_{(1,1)}$ and $\Phi_{(1,0)}$. Inside the harbour, the dynamic component of the free-surface displacement can be split into two parts: the second-order mean free-surface displacement associated with free long waves, and locked long waves. Thus, from (4.3)

$$\zeta^{\mathrm{H}}_{(2,0)} = \tilde{\zeta}^{\mathrm{H}}_{(2,0)} + \hat{\zeta}^{\mathrm{H}}_{(2,0)}, \tag{4.43}$$

where

$$\hat{\zeta}^{\mathrm{H}}_{(2,0)} = -\frac{1}{g} \frac{\partial}{\partial T} \hat{\Phi}^{\mathrm{H}}_{(1,0)} \quad (z = 0), \tag{4.44}$$

$$\begin{aligned}\tilde{\zeta}^{\mathrm{H}}_{(2,0)} = -\frac{1}{g} \Bigg[& \frac{\partial}{\partial T} \tilde{\Phi}^{\mathrm{H}}_{(1,0)} + \overline{\left| \frac{\partial}{\partial x} \Phi^{\mathrm{H}}_{(1,1)} \right|^2} + \overline{\left| \frac{\partial}{\partial y} \Phi^{\mathrm{H}}_{(1,1)} \right|^2} \\ & + \overline{\left| \frac{\partial}{\partial z} \Phi^{\mathrm{H}}_{(1,1)} \right|^2} - \frac{\omega^2}{g} \overline{\left(\Phi^{\mathrm{H}}_{(1,1)} \frac{\partial}{\partial z} \Phi^{\mathrm{H}}_{(1,-1)} + * \right)} \Bigg] \quad (z = 0).\end{aligned} \tag{4.45}$$

After some manipulations, the mean free surface can be written explicitly as

$$\begin{aligned}\hat{\zeta}^{\mathrm{H}}_{(2,0)} = -\sum_{n=1}^{2N} \sum_{q=0}^{\infty} \Bigg\{ & \frac{\mathrm{i}n\omega_0 \mathfrak{G}}{g(C_{\mathrm{g}}^2 - gh)} \lambda_{0n} \frac{\epsilon_q \cos[\mathscr{K}_{qn}(X + \epsilon L)]}{\epsilon B \mathscr{K}_{qn} \sin(\epsilon \mathscr{K}_{qn} L)} \\ & \times \cos(\beta_{0q} Y) \cos(\beta_q y_0)\, J_0(\beta_0 a) \Bigg\} \exp(-\mathrm{i}n\omega_0 T) + *,\end{aligned} \tag{4.46}$$

where $\mathfrak{G}$ is given by (4.8), and

$$\tilde{\zeta}^{\mathrm{H}}_{(2,0)} = \sum_{n=1}^{2N}\sum_{q=0}^{Q}\left\{\frac{4p_{qn}}{g\epsilon_q}\left[\frac{C_{g_q}\mathscr{D}_q}{(C^2_{g_q}-gh)}-\mathscr{D}'\right]\cos\left[nk_{0q}(X+\epsilon L)\right]\exp\left(-in\omega_0 T\right)+*\right\}, \quad (4.47)$$

where

$$\mathscr{D}' = \frac{g^2k^2}{2\omega^2}(1-\tanh^2 kh). \quad (4.48)$$

The steady-state component of the second-order free-surface displacement can be obtained from (4.3) or by taking the limit of (4.43) for uniform incident waves, $\omega_0 = 0$. The details of the steady set-down will not be discussed here.

5. Numerical examples

In this section we consider an incident wave group which consists of two colinear short waves with slightly different frequencies, ω_1 and ω_2. The corresponding wavenumbers are k_1 and k_2, respectively. For simplicity we further assume that the amplitudes of the wave components are the same. The wave envelope of the incident wave group can be written as

$$A^{\mathrm{I}} = \sum_{n=-N}^{N} A^{\mathrm{I}}_n \exp\left[in(\Psi^{\mathrm{I}}-\omega_0 T)\right] = A\cos\left(\Psi^{\mathrm{I}}-\omega_0 T\right), \quad (5.1)$$

where

$$\left.\begin{aligned} A^{\mathrm{I}}_1 = A^{\mathrm{I}}_{-1} = \tfrac{1}{2}A, \quad A^{\mathrm{I}}_n = A^{\mathrm{I}}_{-n} = 0 \quad \text{for } n \neq 1, \\ 2\epsilon k_0 = k_1-k_2, \quad 2\epsilon\omega_0 = \omega_1-\omega_2, \quad 2k = k_1+k_2, \end{aligned}\right\} \quad (5.2)$$

and Ψ^{I} is defined in (3.10). The first-order, first-harmonic potential can be completed by substituting (5.1) and (5.2) into (3.11) and (3.17). From (4.15) the Fourier coefficients for $|A^{\mathrm{I}}|^2$ can be expressed as

$$C_n = \begin{cases} 0, & \text{for } n \neq 2 \\ \frac{1}{4}A^2, & \text{for } n = 2. \end{cases} \quad (5.3)$$

Using (5.3) in (3.21) and (4.30), we obtain

$$p_{q0} = \frac{\epsilon_q^2 A^2}{4B^2}\left\{\left|\frac{\mathscr{G}_q(k_1)}{k_{q1}\sin\left(k_{q1}L\right)}\right|^2 + \left|\frac{\mathscr{G}_q(k_{-1})}{k_{q-1}\sin\left(k_{q-1}L\right)}\right|^2\right\}, \quad (5.4a)$$

$$p_{q1} = 0, \quad (5.4b)$$

$$p_{q2} = \frac{\epsilon_q^2\mathscr{G}_q(k_1)\mathscr{G}_q^*(k_{-1})A^2}{4k_{q1}k^*_{q-1}B^2\sin\left(k_{q1}L\right)\sin^*\left(k_{q-1}L\right)}, \quad (5.4c)$$

with

$$k_{q1} = (k_1^2-\beta_q^2)^{\frac{1}{2}}, \quad k_{q-1} = (k_{-1}^2-\beta_q^2)^{\frac{1}{2}}, \quad k_1 = k+\epsilon k_0, \quad k_{-1} = k-\epsilon k_0, \quad (5.4d)$$

where * denotes the complex conjugate. Substituting (5.3) and (5.4) into (4.39), (4.41), and (4.42), we find

$$\lambda_{0n} = \begin{cases} 0, & \text{for } n \neq 2 \\ \dfrac{\mathbb{N}_2}{\mathbb{D}_2}, & \text{for } n = 2, \end{cases} \quad (5.5)$$

where
$$\mathbb{N}_2 = \tfrac{1}{2}A^2 \exp(2ik_0 \epsilon y_0 \sin\theta_{\mathrm{I}}) - \sum_{q=0}^{Q} \frac{2\mathscr{D}_q}{\epsilon_q} \frac{2p_{q2}}{C_{g_q}^2 - gh} \times \frac{C_g^2 - gh}{\mathfrak{G}} \frac{k_0}{k_{0q}} \cos(2\epsilon k_{0q} L) + 2ik_0 \frac{C_g^2 - gh}{\mathfrak{G}} \sum_{q=0}^{Q} \frac{2\mathscr{D}_q}{\epsilon_q} \times \frac{2i\epsilon B p_{q2}}{C_{g_q}^2 - gh} \sin(2\epsilon k_{0q} L) \left[-\tfrac{1}{2}i + \frac{1}{\pi} \ln(\tfrac{1}{2}\nu\epsilon\alpha k_0 a) \right], \tag{5.6}$$

$$\mathbb{D}_2 = -2ik_0 \left\{ \sum_{q=0}^{\infty} \frac{\epsilon_q}{\epsilon B \mathscr{K}_{q2}} \cot(\epsilon \mathscr{K}_{q2} L) \cos^2(\beta_q y_0) J_0^2(\beta_q a) - \tfrac{1}{2}i \left[1 + \frac{2i}{\pi} \ln(\tfrac{1}{2}\nu\epsilon\alpha k_0 a) \right] \right\}. \tag{5.7}$$

From (4.29) and (4.31) the locked and free long waves inside the harbour can be expressed as

$$\tilde{\Phi}^{\mathrm{H}}_{(1,0)} = \sum_{q=0}^{Q} \left\{ -i \frac{2\mathscr{D}_q}{k_{0q} \epsilon_q} \frac{p_{q2}}{C_{g_q}^2 - gh} \cos[2k_{0q}(X + \epsilon L)] \exp(-2i\omega_0 T) + * \right\}, \tag{5.8}$$

$$\hat{\Phi}^{\mathrm{H}}_{(1,0)} = -\frac{\mathfrak{G}}{C_g^2 - gh} \lambda_{02} \sum_{q=0}^{\infty} \frac{\epsilon_q \cos[\mathscr{K}_{q2}(X + \epsilon L)]}{\epsilon B \mathscr{K}_{q2} \sin(\epsilon \mathscr{K}_{q2} L)} \cos(\beta_{0q} Y) \times \cos(\beta_q y_0) J_0(\beta_q a) \exp(-2i\omega_0 T) + *. \tag{5.9}$$

The corresponding second-order dynamic free-surface displacement can be expressed as

$$\hat{\zeta}^{\mathrm{H}}_{(2,0)} = -\sum_{q=0}^{\infty} \left\{ \frac{2i\omega_0 \mathfrak{G}}{g(C_g^2 - gh)} \lambda_{02} \frac{\epsilon_q \cos[\mathscr{K}_{q2}(X + \epsilon L)]}{\epsilon B \mathscr{K}_{q2} \sin(\epsilon \mathscr{K}_{q2} L)} \times \cos(\beta_{0q} Y) \cos(\beta_q y_0) J_0(\beta_q a) \right\} \exp(-2i\omega_0 T) + *, \tag{5.10}$$

$$\tilde{\zeta}^{\mathrm{H}}_{(2,0)} = \sum_{q=0}^{Q} \left\{ \frac{4p_{q2}}{g\epsilon_q} \left[\frac{C_{g_q} \mathscr{D}_q}{C_{g_q}^2 - gh} - \mathscr{D}' \right] \times \cos[2k_{0q}(X + \epsilon L)] \exp(-2i\omega_0 T) + * \right\}. \tag{5.11}$$

For convenience, the second-order free-surface displacement can be written as

$$\zeta^{\mathrm{H}}_{(2,0)} = \hat{\zeta}^{\mathrm{H}}_{(2,0)} + \tilde{\zeta}^{\mathrm{H}}_{(2,0)} = (\hat{A}^{\mathrm{H}}_{(2,0)} + \tilde{A}^{\mathrm{H}}_{(2,0)}) \exp(-2i\omega_0 T) + *. \tag{5.12}$$

The amplitude of the second-order free-surface displacement can be defined as

$$A^{\mathrm{H}}_{(2,0)} = 2|\hat{A}^{\mathrm{H}}_{(2,0)} + \tilde{A}^{\mathrm{H}}_{(2,0)}|, \tag{5.13}$$

which can be normalized as

$$A^{\mathrm{H}}_{(2,0)} = \frac{A^{\mathrm{H}}_{(2,0)}}{2kA^2 \mathbb{R}(kh)}, \tag{5.14}$$

where
$$\mathbb{R}(kh) = \frac{C_g(2C + C_g - \gamma^2 C_g)}{\gamma(C_g^2 - gh)}. \tag{5.15}$$

Note that $\mathbb{R}(kh)$ is a function of kh only and increases monotonically as kh decreases (see figure 2).

From (5.9) and (5.10), the free long waves start to resonate as $(\epsilon \mathscr{K}_{q2} L)$ approaches $n\pi$, where $n = 0, 1, 2, \ldots$. According to the definitions given in (4.32), this implies that when the wavenumber of free long waves is close to one of the natural modes of the

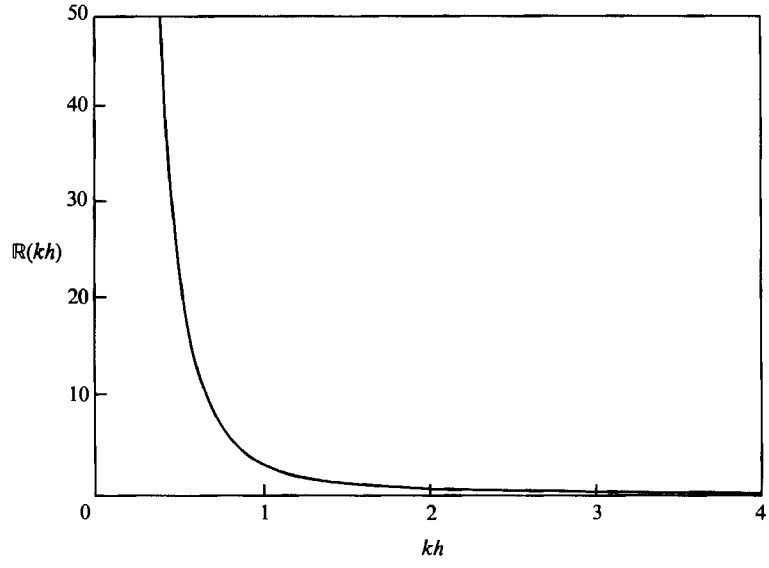

FIGURE 2. The depth function $\mathbb{R}(kh)$.

closed basin, $(2\alpha\epsilon k_0) = [(n\pi/L)^2 + (q\pi/B)^2]^{\frac{1}{2}}$, resonance should be expected. A more accurate estimation of the resonant wave envelope wavenumber can be obtained from a simple perturbation analysis (Ünlüata & Mei 1973). In the neighbourhood of the natural modes of the closed basin we assume

$$(2\alpha\epsilon k_0)_{nq} = (k_0)_{nq} + \Delta, \tag{5.16a}$$

and

$$(k_0)_{nq} = \left[\left(\frac{n\pi}{L}\right)^2 + \left(\frac{q\pi}{B}\right)^2\right]^{\frac{1}{2}}, \quad \Delta \ll (k_0)_{nq}. \tag{5.16b}$$

Substitution of (5.16) into (5.9) or (5.10) yield an approximate solution for Δ at resonance. The procedure is straightforward and can be found in Mei (1983) for short waves and in Wu (1988) for long waves. The details of this analysis are omitted here; only the results are presented. Thus, for non-Helmholtz modes, i.e. $n \neq 0$ and $q \neq 0$,

$$\Delta = -\frac{\mathbb{A}}{\mathbb{B}}, \tag{5.17a}$$

$$\mathbb{A} = \frac{\epsilon_n \epsilon_q}{2(k_0)_{nq} BL} \cos^2(\beta_q y_0) J_0^2(\beta_q a), \tag{5.17b}$$

$$\mathbb{B} = \sum_{\substack{j=0 \\ j \neq q}}^{\infty} \frac{\epsilon_j \cos(\mathscr{K}_{j2} \epsilon L)}{\mathscr{K}_{j2} \epsilon B \sin(\mathscr{K}_{j2} \epsilon L)} \cos^2(\beta_j y_0) J_0^2(\beta_j a) + \frac{1}{\pi} \ln(\tfrac{1}{4}\nu(k_0)_{nq} a), \tag{5.17c}$$

in which $\mathscr{K}_{j2}$ is defined in (4.32). Near the Helmholtz mode, Δ is the root of the following equation:

$$\Delta^2 LB \ln(\tfrac{1}{4}\nu\Delta a) + \pi = 0. \tag{5.18}$$

Numerical computations are performed for a square harbour basin ($B/L = 1.0$) with normal incident waves ($\theta_1 = \pi$). The following two sets of parameters are used in computations: (*a*) $kh = 0.5$, $kL = 20$, $a/B = 0.1$, $y_0/B = 0.5$, and (*b*) $kh = 0.5$, $kL = 40$, $a/B = 0.2$, $y_0/B = 0.5$. In the second case the harbour entrance is much

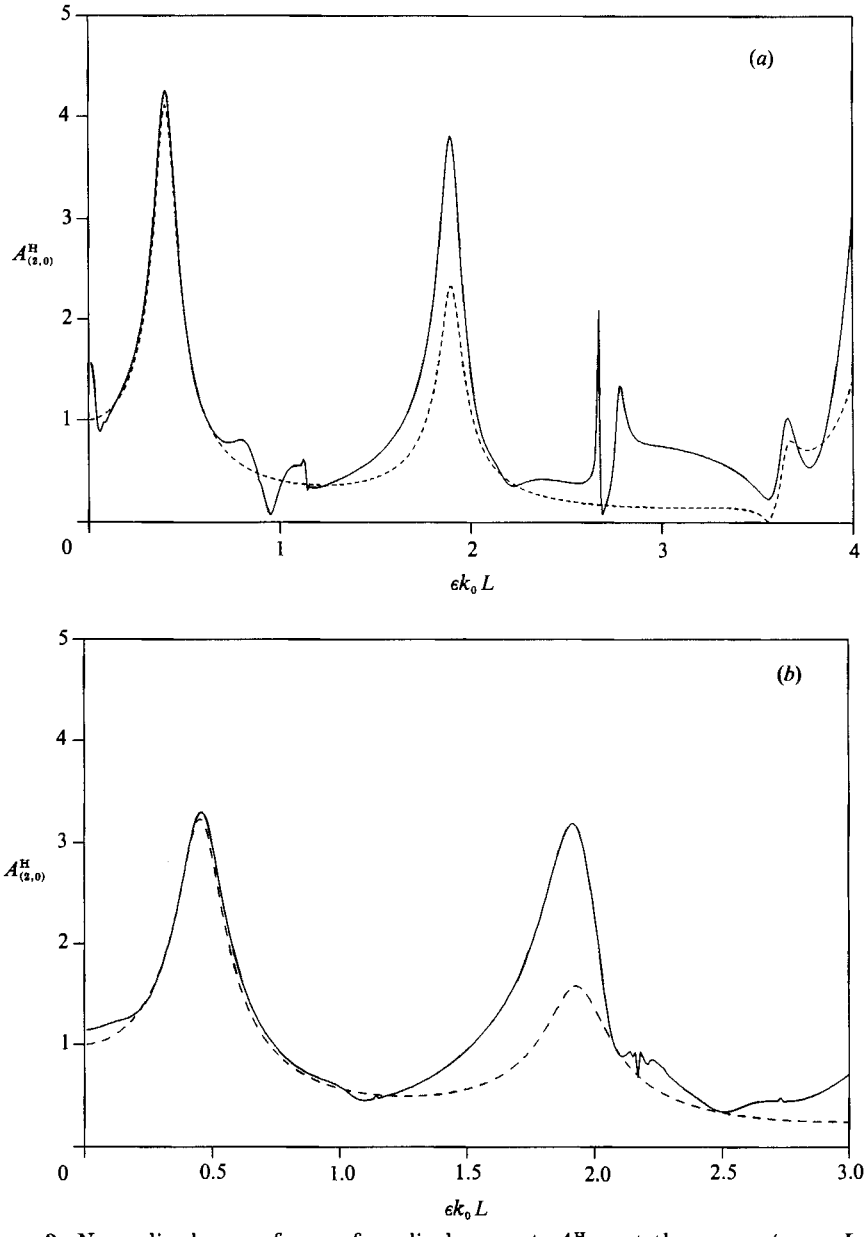

FIGURE 3. Normalized mean free-surface displacement, $A^{H}_{(2,0)}$, at the corner $(x = -L, y = 0)$ of a square harbour as a function of the normalized wavenumber of the incident wave group, $\epsilon k_0 L$. The following parameters are used: (*a*) $kh = 0.5$, $kL = 20$, $B/L = 1.0$, $a/B = 0.1$, $y_0/B = 0.5$, $\theta_I = \pi$; and (*b*) $kh = 0.5$, $kL = 40$, $B/L = 1.0$, $a/B = 0.2$, $y_0/B = 0.5$, $\theta_I = \pi$. ——, Complete solution; – – –, without the locked long waves inside the harbour.

wider than that of the first case. In figure 3 the normalized second-order free-surface displacements, $A^{H}_{(2,0)}$, at the corner of the harbour $(x = -L, y = 0)$ are plotted for different values of the normalized wavenumber for wave groups, $\epsilon k_0 L$. The first resonant peak, corresponding to the Helmholtz mode, occurs at $\epsilon k_0 L = 0.396$ for the first case, and at $\epsilon k_0 L = 0.445$ for the second case with a wider harbour entrance. The lowest three resonant wavenumbers predicted by (5.17) and (5.18) and numerical

Modes	Approximated theoretical results (5.17), (5.18)	Numerical solutions
(*a*)		
$n = 0, q = 0$	0.389	0.396
$n = 1, q = 0$	1.932	1.897
$n = 2, q = 0$	3.643	3.660
(*b*)		
$n = 0, q = 0$	0.66	0.45
$n = 1, q = 0$	2.10	1.93
$n = 2, q = 0$	4.33	3.96

TABLE 1. Resonant wavenumbers of the incident wave envelope, $\epsilon k_0 L$. (*a*) $kh = 0.5$, $kL = 20$, $B/L = 1.0$, $a/B = 0.1$, $y_0/B = 0.5$, and $\theta_I = \pi$; (*b*) $kh = 0.5$, $kL = 40$, $B/L = 1.0$, $a/B = 0.2$, $y_0/B = 0.5$, and $\theta_I = \pi$

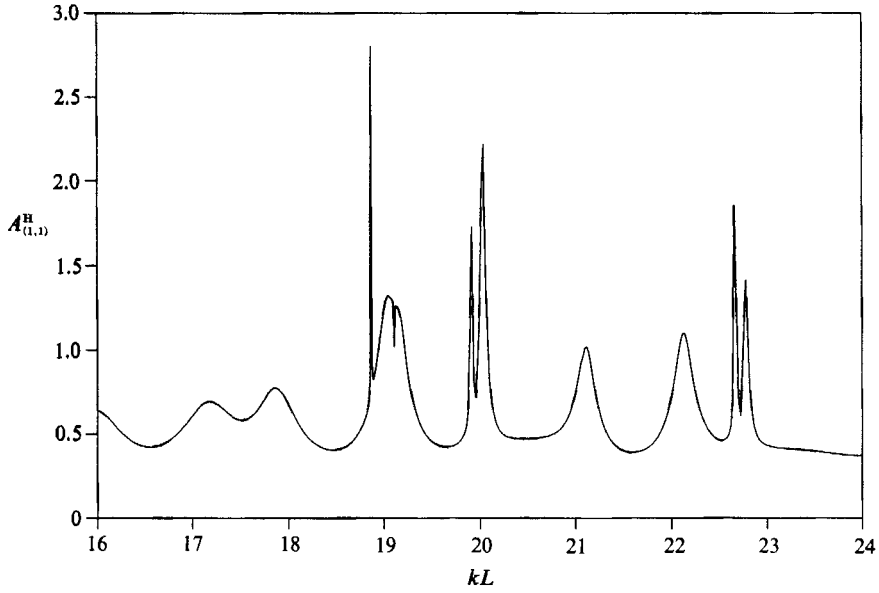

FIGURE 4. Harbour response for the first-order waves, $A^{H}_{(1,1)}$, as a function of the normalized carrier wavenumber, kL. The following parameters are: $kh = 0.5$, $B/L = 1.0$, $a/B = 0.1$, $y_0/B = 0.5$.

solutions are listed in table 1 for both cases. The approximated analytical results agree with the numerical solutions very well for the first case, but not so well for the second case. This is because the approximated analytical solutions are based on the approximation that the harbour entrance is small in comparison with the dimension of the harbour basin.

For purposes of comparison, numerical results are also obtained for the problems in which the locked long waves inside the harbour are artificially ignored. (The free long waves inside the harbour are obtained by using the matching conditions (4.33) and (4.34) without the locked long wave terms, $\hat{\Phi}^{H}_{(1,0)}$.) The differences in these numerical results are rather small for $\epsilon k_0 L < 1.0$, indicating that the locked long waves inside the harbour might not be important in evaluating the second-order dynamic free-surface responses within this range of frequencies. For the first case with a smaller harbour entrance the seconday peaks appearing in the full solution

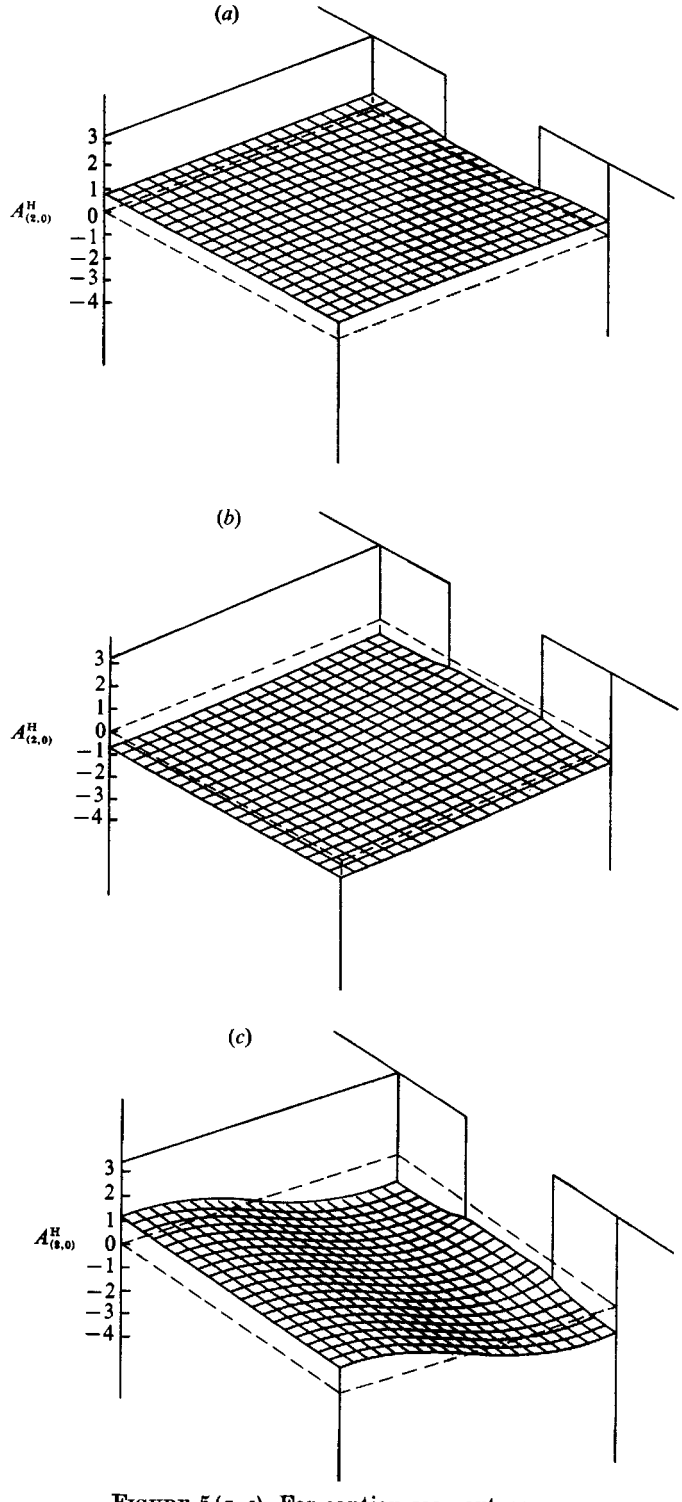

FIGURE 5(*a–c*). For caption see next page.

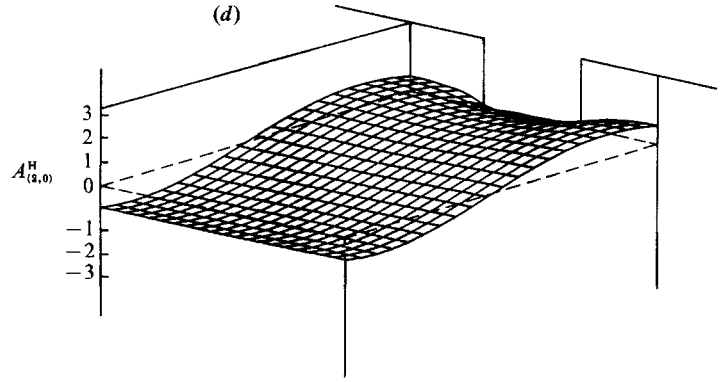

FIGURE 5. Snapshots of the mean free-surface displacements inside the square harbour as described in figure 3(*b*) near two resonant wavenumbers: (*a*) $\epsilon k_0 L = 0.445$, $2\omega_0 t_1 = 0$; (*b*) $\epsilon k_0 L = 0.445$, $2\omega_0 t_1 = \pi$; (*c*) $\epsilon k_0 L = 1.92$, $2\omega_0 t_1 = 0$; (*d*) $\epsilon k_0 L = 1.92$, $2\omega_0 t_1 = \pi$.

(solid line in figure 3*a*) correspond to the resonant peaks of the carrier (short) waves. To illustrate this point more clearly, we define the normalized first-order harbour response as

$$A^{H}_{(1,1)} = \frac{1}{A}\left[\frac{1}{BL}\int_{-L}^{0}\int_{0}^{B} |\zeta_{(1,1)}|^2 \,\mathrm{d}x\,\mathrm{d}y\right]^{\frac{1}{2}}. \tag{5.19}$$

In figure 4 the first-order harbour responses are plotted using the same set of geometrical parameters as for the first case. Because the incident waves are the superposition of two short-wave components, $k \pm \epsilon k_0$, the incident short waves are resonated at $(k \pm \epsilon k_0)L \approx (19.95, 20.05)$, $(18.9, 21.1)$, and $(17.2, 22.7)$. For $kL = 20$ these four sets of resonant frequencies correspond to $\epsilon k_0 L \approx 0.05$, 1.1, and 2.7. For the second case where the harbour entrance is much larger than the short wavelength the influence of the short-wave resonance on the long-wave responses is relatively weak within the given range of $\epsilon k_0 L$.

In figure 5 the mean free-surface displacements inside the harbour near the first resonant frequencies ($\epsilon k_0 L = 0.445$ and 1.92) of the second case with a larger harbour entrance are plotted. The mean free-surface displacements are shown at $2\omega_0 t_1 = 0$ and π. Near the first resonance (Helmholtz) mode, the free-surface displacements are more or less uniform inside the harbour except in the vicinity of the harbour mouth. At the second resonance mode, the second-order mean free-surface displacements behave as a standing wave in the x-direction.

Numerical results have also been obtained for different harbour shapes, i.e. $B \neq L$, and for different locations of the harbour mouth. The response curves for the second-order mean free-surface displacements for different harbour geometry are similar to figure 3 and will not be reported here; the detailed results can be found in Wu (1988).

6. Concluding remarks

Assuming that the water depth is a constant and the coastline is a straight line, we obtained analytical solutions for the second-order long-wave oscillations in a rectangular harbour basin, excited by incident wave groups. It is shown that although both locked and free long waves exist inside the harbour basin, the

reponses in the neighbourhood of the lowest resonant mode are dominated by free long waves. The locked long waves could be ignored for all practical purposes. Since it is extremely difficult to calculate the locked long waves inside a harbour basin with an arbitrary shape and a varying depth, this conclusion could simplify the matter significantly.

It should be reiterated here that because of the simplifying assumptions used in defining the geometry of the harbour, topography, and the shoreline configuration, important physical features such as shoaling and refraction outside the harbour, the energy losses due to flow separation near the harbour entrance and wave breaking nearshore are not considered. Future research should include some or all of these features.

The research reported here was supported by the New York Sea Grant Institute through a research grant to Cornell University. The manuscript was written when P. L.-F. Liu was a Visiting Professor at the Technical University of Denmark. The financial support from the University is appreciated. Discussions with J. K. Kostense and reviewers' comments were also very helpful.

REFERENCES

AGNON, Y. & MEI, C. C. 1985 Slow-drift motion of a two-dimensional block in beam seas. *J. Fluid Mech.* **151**, 279–294.

AGNON, Y. & MEI, C. C. 1988 Trapping and resonance of long shelf waves due to groups of short waves. *J. Fluid Mech.* **195**, 201–222.

BOWERS, E. C. 1977 Harbour resonance due to set-down beneath wave groups. *J. Fluid Mech.* **79**, 71–92.

LIU, P. L.-F. 1989 A note on long waves induced by short-wave groups over a shelf. *J. Fluid Mech.* **205**, 163–170.

LIU, P. L.-F., DINGEMANS, M. W. & KOSTENSE, J. K. 1990 Long waves generation due to the refraction of short-wave groups over a shear current. *J. Phys. Oceanogr.* **20**, 53–59.

LONGUET-HIGGINS, M. S. & STEWART, R. W. 1962 Radiation stress and mass transport in gravity waves, with applications to 'surf beats'. *J. Fluid Mech.* **13**, 481–504.

MEI, C. C. 1983 *The Applied Dynamics of Ocean Surface Waves.* Wiley-Interscience.

MEI, C. C. & AGNON, Y. 1989 Long-period oscillations in a harbour induced by incident short waves. *J. Fluid Mech.* **208**, 595–608.

MEI, C. C. & BENMOUSSA, C. 1984 Long waves induced by short-wave groups over an uneven bottom. *J. Fluid Mech.* **139**, 219–235.

MILES, J. W. & MUNK, W. 1961 Harbor paradox. *J. Waterways and Harbor Div. ASCE* **87**, 111–130.

MOLIN, B. 1982 On the generation of long-period second-order free-waves due to changes in the bottom profile. *Papers of the Ship Research Institute, Tokyo, Japan* 68.

ÜNLÜATA, Ü. & MEI, C. C. 1973 Long wave excitation in harbors – an analytical study. *Tech. Rep.* 171. *Dept. of Civil Engineering, M.I.T.*

WU, J.-K. 1988 Low-frequency harbor resonance. Doctoral thesis, School of Civil and Environmental Engineering, Cornell University.

ZHOU, C. & LIU, P. L.-F. 1987 Second-order low-frequency wave forces on a vertical cylinder. *J. Fluid Mech.* **175**, 143–155.